Hydrocalumite and Its Polymer Derivatives. 2. Polymer Incorporation versus in Situ Polymerization of Styrene-4-sulfonate

Laetitia Vieille, Christine Taviot-Guého, Jean-Pierre Besse, and Fabrice Leroux*

Laboratoire des Matériaux Inorganiques, UMR 6002, Université Blaise Pascal, 63177 Aubière Cédex, France

Received April 8, 2003. Revised Manuscript Received July 23, 2003

Hydrocalumite, $Ca_2Al(OH)_6(anion)\cdot nH_2O$, belongs to the layered double-hydroxide family, with the particularity for both intralayered cations and interlayered anions and water molecules to be well-ordered. The monomer vinyl benzene sulfonate (VBS) and the syndiotactic polymer poly(styrene sulfonate) (PSS) were readily incorporated into its lamellar structure via a coprecipitation method. In situ thermal polymerization of the monomer VBS is simultaneously supported by the disappearance of the vinyl bond and the formation of $-CH$, $-CH_2$ bonds. These facts are evidenced by the experiments performed by ^{13}C solid-state NMR and FTIR spectroscopies. CaAl−VBS intercalate crystallizes in the *C*2/*c* space group, inducing a bilayer arrangement of VBS anions in the interlamellar space. Besides, distances between anionic sites allow an in situ zigzag polymerization of syndiotactic type along the *a* axis. Additionally, the contraction of the lamellar structure is found to be reversible up to 200 °C; the adjacent monomers then start to attach to each other via polymerization. The thermal stability is found to be highly dependent on the synthesis pathway. The decomposition is delayed up to 450 °C for the sample prepared via in situ polymerization while as-prepared PSS intercalate decomposes at lower temperature. Under a nitrogen atmosphere, CaS is formed at 700 °C.

1. Introduction

In the past 2 decades, much research has been devoted to the inorganic−organic polymer assembly.[1] Because it may reproduce to some extent the formation of biogenic materials, such as marine organisms, the study of organo-silicas[2] or organoceramics[3] are of great interest to better understand the intricacy of such systems. In this way, it has been found that the presence of polymer may drastically modify the morphology of calcium oxalate crystals.[4] Another approach is to take advantage of the presence of the two components and to combine their properties. For example, the size of cobalt nanoparticles may be physically restricted in the pores of hyper-cross-linked polystyrene.[5]

In the present work, we focus our attention on hydrocalumite of composition $Ca_2Al(OH)_6X\cdot nH_2O$ (X = anion), noted as Ca_2Al/X, as the host structure. Few papers report the incorporation of organics into hydrocalumite.[6] A companion paper has presented the characterization of Ca_2Al/Cl and its behavior in temperature.[7] Layered double hydroxides are predominantly hydrotalcite-like materials, which are a random distribution of the cations within the hydroxide layers. On the other hand, the hydrocalumite structure is completely ordered. Aluminum atoms are 6-fold coordinated, whereas the calcium atoms present a [6+1]-coordination, the seventh apex oxygen atom coming from the interlayer water molecule.[8]

The incorporation of polymer into a hydrocalumite host is of current concern for cement application. Indeed, like calcium silicate (noted as C−S−H), these calcium aluminum hydroxide salts called Friedel salts occur in the hydration process of cement and their role in the mechanical properties is of major importance.[9]

It was shown that the filling of the large voids present initially within the cement was a key factor to reinforce the whole structure.[10] Those materials are defined as Macro Defect Free cements.[11] From a theoretical approach,[12] it was demonstrated that the cross-linking of

* To whom correspondence should be addressed. E-mail: fleroux@chimtp.univ-bpclermont.fr.

(1) Special Issue of *Chemistry of Materials*: Organic−Inorganic Nanocomposite Materials 2001, Vol. 13. Ruiz-Hitzky, E. *Adv. Mater.* **1993**, *5*, 334. Giannelis, E. P. *Adv. Mater.* **1996**, *8*, 29. Novak, B. M. *Adv. Mater.* **1993**, *5*, 422. Harreld, J. H. B.; Dunn, B.; Nazar, L. F. *Int. J. Inorg. Mater.* **1999**, *1*, 135. Portier, J.; Choy, J.-H.; Subramanian, M. A. *Int. J. Inorg. Mater.* **2001**, *3*, 581. Leroux, F.; Besse, J.-P. *Chem. Mater.* **2001**, *13*, 3507.

(2) Asefa, T.; Yoshina-Ishii, C.; MacLachlan, M. J.; Ozin, G. A. *J. Mater. Chem.* **2000**, *10*, 1751.

(3) Berman, A.; Addadi, L.; Weiner, S. *Nature* **1988**, *331*, 546.

(4) Zhang, D.; Qi, L.; Ma, J.; Cheng, H. *Chem. Mater.* **2002**, *14*, 2457

(5) Sidorov, S. N.; Bronstein, L. M.; Davznkov, V. A.; Tsyurupa, M. P.; Solodovnikov, S. P.; Valetsky, P. M. *Chem. Mater.* **1999**, *11*, 3210.

(6) Dekany, I.; Berger, F.; Imrik, K.; Lagaly, G. *Colloid Polym. Sci.* **1997**, *275*, 681. Meyn, M.; Beneke, K.; Lagaly, G. *Inorg. Chem.* **1990**, *29*, 5201. Khan, A. I.; O'Hare, D. *J. Mater. Chem.* **2002**, *12*, 3191.

(7) Vieille, L.; Rousselot, I.; Leroux, F.; Besse, J.-P.; Taviot-Guého, C. *Chem. Mater.* **2003**, *15*, 4361−4368.

(8) Lopez-Salinas, E.; Llanos Serrano, M. E.; Cortés Jacome M. A.; Schifter Secora, I. *J. Porous Mater.* **1996**, *2*, 291. Ahmed, S. J.; Taylor, H. F. W. *Nature* **1967**, *215*, 622. Rousselot, I.; Taviot-Guého, C.; Leroux, F.; Léone, P.; Palvadeau, P.; Besse, J.-P. *J. Solid State Chem.* **2002**, *167*, 137 and references therein.

(9) Fernon, V.; Vichot, A.; Colombet, P.; van Damme, H.; Béguin, F. *Mater. Sci. Forums* **1994**, *152−153*, 335. Kuzel, H.; Baier, H. *Eur. J. Miner.* **1996**, *8*, 129.

10.1021/cm031070i CCC: $25.00
Published on Web 10/22/2003

polymer chains, polyacrylate (PPA) and polyvinylalcool (PVA), with either Ca or Al atoms could be done via the carboxylate and the terminaison −O−, respectively. In some cases, the mechanical properties were achieved when the polymer was truly intercalated between the layers.[13]

Recent work has shown that CSH layers do not expand upon polymer incorporation, probably yielding to an entanglement rather than to a true intercalation.[14]

Conversely, the calcium aluminum hydroxide presents a large anionic exchange capacity, making almost any exchange reaction possible. In this way, the incorporation of poly(vinyl alcohol) (PVA) between the layers of the hydrocalumite has been reported.[15] The assembly was realized via coprecipitation; the microtextural property was modified, the polymer acting as a bridge between the platelet-like structure and retarding the decomposition of the inorganic layers.

The system PSS/hydrotalcite-related nanocomposites has previously been reported.[16] We show here the incorporation and subsequent polymerization of styrene-4-sulfonate (VBS) and poly(styrene sulfonate) (PSS) into hydrocalumite. Such an in situ thermal polymerization of pre-intercalated monomers has also been observed for aspartate into Mg_2Al,[17] aniline sulfonate into Cu_2Cr,[18] and recently for VBS into Zn_2Al.[19] Yet several questions remain on the incorporation of polymer between the sheets of hydrotalcite. In a parent organoceramic material Zn_2Al/VBS, the polymerization was found to occur when a good matching between the charge density of the LDH material and the size of VBS was present.[19] The ordered cation repartition within the lamellae and the peculiar environment of Ca^{2+} induce an order in the gap of hydrocalumite, contrary to most synthetic hydrotalcite compounds. In this respect, hydrocalumite can serve as a model for less ordered LDH. On the basis of structural considerations, a simple model is proposed to modelize the reaction of polymerization of VBS into the hydrocalumite gap.

The stability in temperature of the organoceramic materials was investigated by XRD measurements and ^{27}Al solid-state NMR spectroscopy.

2. Experimental Section

2.1. Syntheses of the Organic Derivatives. The preparation of the hydrocalumite Ca_2Al/Cl was described in a companion paper.[7] The incorporation of sodium styrene-4-sulfonate (Fluka, >90%) and sodium poly(styrene-4-sulfonate) (M_w = 70000, Acros) was carried out using the "organized assembly" approach;[16] that is, during the coprecipitation, an excess of 5 equiv of organic anion over Al^{3+} content was used. Typically, 20 mL of a solution containing a mixture of $CaCl_2$ (0.66 M) and $AlCl_3$ (0.33 M) is added dropwise under a nitrogen atmosphere to 250 mL of an aqueous solution in which 5.155 g of organics (VBS or PSS) has been previously dissolved. The conditions for the coprecipitation are rigorously the same (*T*, pH, and aging time) as that for the preparation of the pristine sample Ca_2Al/Cl. The resulting powders were washed several times with decarbonated water and then dried under vacuum.

Table 1. Chemical Analysis of Ca_2Al/Cl and the Organic Derivatives[a]

sample	chemical formulas	*d*-spacing (nm)
Ca_2Al/Cl	$Ca_{0.67}Al_{0.33}(OH)_2Cl_{0.33}\cdot nH_2O$	0.79
Ca_2Al/VBS	$Ca_{0.67}Al_{0.33}(OH)_2(C_8H_7SO_3)_{0.32}\cdot nH_2O$	1.77
Ca_2Al/PSS	$Ca_{0.67}Al_{0.33}(OH)_2(C_8H_7SO_3)_{0.32}\cdot nH_2O$	1.92

[a] The basal spacing is displayed.

Elemental analysis (H, C, S, Ca, and Al) was performed at the Vernaison Analysis Center of CNRS using inductive conduction plasma coupled to atomic emission spectroscopy (ICP/AES). The chemical compositions are reported in Table 1.

In the following, the pristine material and organic derivatives will be written as Ca_2Al/X where X represents the interlayer anion.

2.2. Instrumentation. Powder X-ray diffraction profiles (PXRD) were obtained with an X'Pert Pro Philips diffractometer using Cu Kα radiation and equipped with a HTK16 Anton Paar chamber and a PSD-50m Braun detector (aperture on 2° - 155 channels). In situ temperature XRD measurements are described in the companion paper.

FTIR spectra were recorded on a Perkin-Elmer 2000 FT spectrometer employing the KBr dilution technique.

2.3. Solid-State NMR Spectroscopy. ^{13}C (I = 1/2) and ^{27}Al (I = 5/2) solid-state NMR experiments were performed with a 300 Bruker spectrometer at 75.47 and 78.20 MHz, respectively. For both nuclei, the experiments were carried out using magic angle spinning (MAS) at 10 kHz and a 4-mm-diameter zirconia rotor. ^{13}C spectra obtained by the proton-enhanced cross-polarization method (CP) are referenced to the carbonyl of the glycine calibrated at 176.03 ppm.

For ^{27}Al nuclei, $Al(H_2O)_6^{3+}$ was used as a reference. Short radio frequency pulses associated with a recycling time of 500 ms were used. Chemical shifts are not corrected from the second-order quadrupolar effect, which induces a shift to a lower frequency.[20]

3. Results and Discussion.

3.1. Incorporation and Interaction of the Organics. The chemical compositions are reported in Table 1. For each sample, the molar ratio Ca/Al is close to the expected value, that is, 2.0, indicating that the reaction was complete. For both materials prepared by the *organized assembly* method, the amount of organics, calculated from the sulfur content, is in agreement with what should theoretically be expected from the exchange capacity. It is noteworthy that we were unsuccessful in preparing a pure sample Ca_2Al/X, with either X = VBS or PSS, via an exchange reaction or by reconstruction. In the latter case, the process is available for VBS but not PSS; however, the presence of $CaCO_3$ cannot be avoided.

(10) Popoola, O. O.; Krive, W. M.; Young, J. F. *J. Am. Ceram. Soc.* **1991**, *74*, 1928. Rodger, S. A.; Sinclair, W.; Groves, G. W.; Brooks, S. A.; Double, D. D. *J. Mater. Sci.* **1985**, *20*, 2853.
(11) Birchall, J. D.; Howard, A. J.; Kendall, K. *Nature* **1981**, *289*, 388.
(12) Bonapasta, A. A.; Buda, F.; Colombet, P. *Chem. Mater.* **2000**, *12*, 738. Bonapasta, A. A.; Buda, F.; Colombet, P. *Chem. Mater.* **2001**, *13*, 64. Bonapasta, A. A.; Buda, F.; Colombet, P.; Guerrini, G. *Chem. Mater.* **2002**, *14*, 1016.
(13) Strawhecker, K. E.; Manias, E. *Chem. Mater.* **2000**, *12*, 2943.
(14) Merlin, F.; Lombois, H.; Joly, S.; Lequeux, N.; Halary, J.-L.; Van Damme, H. *J. Mater. Chem.* **2002**, *12*, 3308.
(15) Messersmith, P. B.; Stupp, S. I. *Chem. Mater.* **1995**, *7*, 454.
(16) Oriakhi, C. O.; Farr, I. V.; Lerner, M. M. *Clays Clay Miner.* **1997**, *45*, 194. Wilson, O. C., Jr.; Olorunyolemi, T.; Jaworski, A.; Borum, L.; Young, D.; Siriwat, A.; Dickens, E.; Oriakhi, C.; Lerner, M. M. *Appl. Clay Sci.* **1999**, *15*, 265. Oriakhi, C. O.; Farr, I. V.; Lerner, M. M. *J. Mater. Chem.* **1996**, *6*, 103.
(17) Whilton, N. T.; Vickers, P. J.; Mann, S. *J. Mater. Chem.* **1997**, *7*, 1623.
(18) Moujahid, El M.; Dubois, M.; Besse, J.-P.; Leroux, F. *Chem. Mater.* **2002**, *14*, 3799.
(19) Moujahid, El M.; Besse, J.-P.; Leroux, F. *J. Mater. Chem.* **2002**, *12*, 3324.
(20) Engelhardt, G.; Michel, D. In *High-Resolution Solid State NMR of Silicates and Zeolites*; Wiley: New York, 1987.

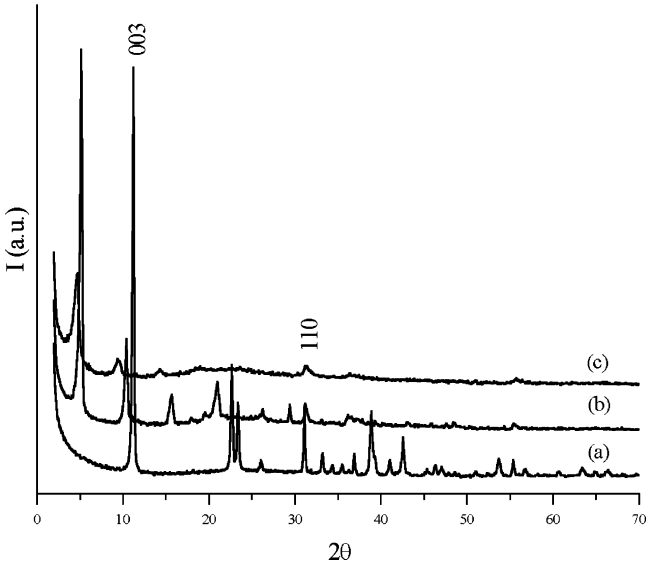

Figure 1. XRD patterns of the hydrocalumite Ca_2Al/X samples, X = Cl (a), VBS (b), and PSS (c). Miller indexing is given for the sample Ca_2Al/Cl.

3.1.1. XRD Study. The structural information relative to the pristine Ca_2Al/Cl sample are presented in a companion paper.[7] The presence of the organic molecules inside the lamellar host is clearly evidenced by the net increase of the basal spacing from 0.79 nm for Ca_2Al/Cl to 1.77 and 1.92 nm for Ca_2Al/VBS and Ca_2Al/PSS, respectively (Figure 1).

An increase in the harmonics (00*l*) width for both organic derivatives is observed, which is likely to be due to a significant disorder in the stacking direction, a phenomenon referred to as turbostatic effects. A large broadening of the diffraction line (110) is also noticed, showing that a partial disorder is occurring within the sheets.

However, in comparison to the ill-organized sample obtained with Zn_2Al, for which a subsequent hydrothermal treatment was necessary to obtain a well-ordered system,[19] the polymer "organized assembly" method gives rise here to a rather well-defined system, demonstrating that the nucleation of the inorganic seed and its subsequent growth is not prevented by the presence of negatively charged polymer.

Considering a layer thickness of 0.202 nm for the layers and the size of the guest molecule of 0.780 nm estimated from electronic Hartree−Fock semiempirical calculation, the space available for VBS is 1.57 nm, indicating a double-layer arrangement for VBS. This aspect will be further discussed in section 3.5. The dimension of the gap (1.51 nm) for Ca_2Al/PSS is also in agreement with the presence of syndiotactic PSS.

3.1.2. NMR Study. ^{13}C solid-state NMR spectra of the samples Ca_2Al/VBS and Ca_2Al/PSS are presented in Figure 2. The spectrum of each organic is also displayed for comparison. The resonance peaks are assigned according to the literature:[21] C^1, δ = 113.9 ppm; C^2, δ = 137.4 ppm; C^3, δ = 141.5 ppm; C^4, δ = 125 ppm; C^5, δ = 143.8 ppm, in $C^1H_2{=}C^2H{-}C^3(C_4{}^4H_4)C^5{-}SO_3(Na)$.

When incorporated between the sheets of Ca_2Al, VBS encounters a large (de)-shielding effect since the resonance peaks of C^2, C^1, C^3, and C^5 carbons atoms are substantially shifted (Figure 2a,c). Indeed, a shielding effect of ≈2 ppm (150 Hz) is observed for C^5 and the position for C^3 and C^2 is shifted of a similar amplitude, whereas C^1 is deshielded (≈215 Hz). These values can be explained by electrostatic interactions between the SO_3 function and the inner surface of the inorganic layers, weakening the electrophilic character toward C^5. Such an effect propagates through the benzene backbone down to C^1 carbon atoms, which is shifted to downfield values. The shifts are of the same amplitude as those observed for VBS incorporated between the layers of Zn_2Al or Mg_2Al.[19]

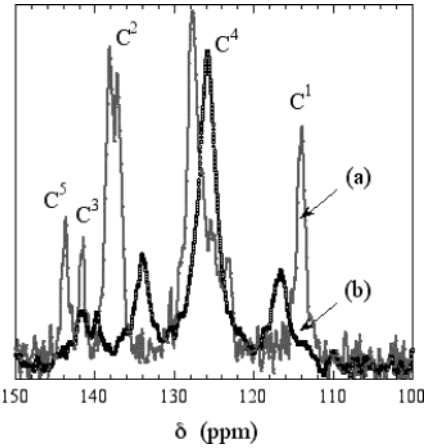

Figure 2. ^{13}C CP-MAS spectra of (a) VBS molecule and of (b) Ca_2Al/VBS. See text for the assignments.

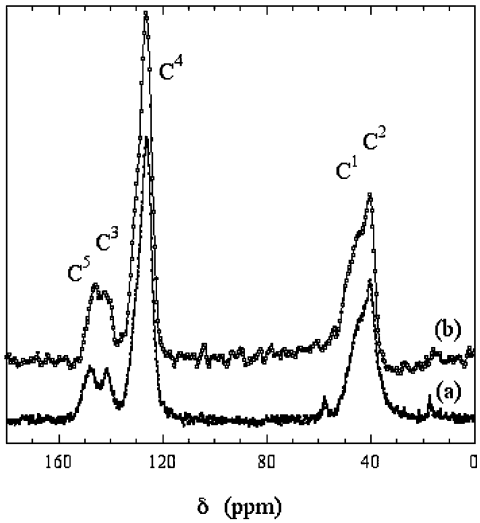

Figure 3. ^{13}C CP-MAS spectra of (a) polymer PSS and of (b) Ca_2Al/PSS.

For the polymer spectrum, the chemical shifts are different, consistent with the absence of the vinyl bond. C^1 and C^2 are observed at large upfield values (Figure 3a).

At a first glance, the ^{13}C CP-MAS spectrum of Ca_2Al/PSS resembles the one obtained for PSS (Figure 3); however, the chemical shift for the C^5 carbon atom is slightly changed. It corresponds to a shielding effect like the one evidenced for the molecule VBS, though less intense. This suggests that the polymer interacts with the layers of Ca_2Al, but not as strongly as in the case of interleaved monomers.

(21) Geismar, G.; Lewandowski, J.; de Boer, E. *Chem.-Ztg.* **1991**, *115*, 335.

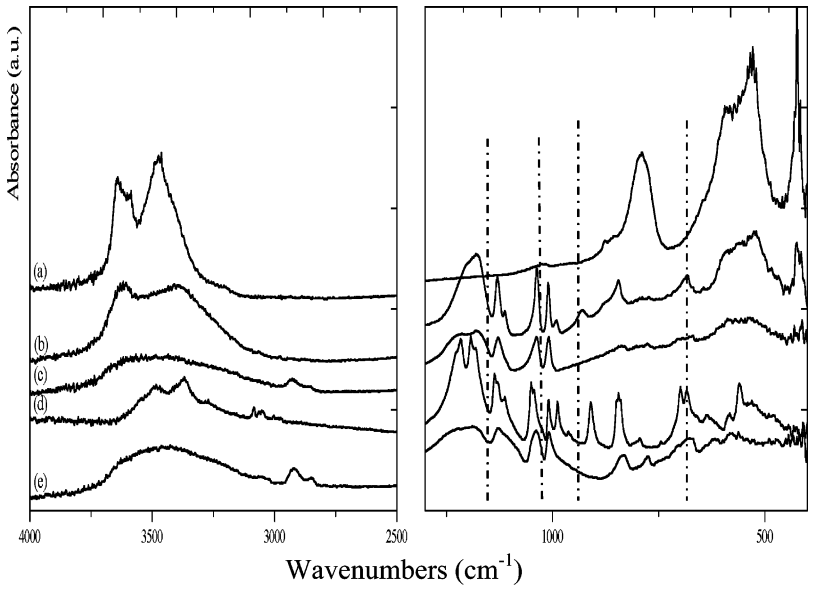

Figure 4. Regions of interest of the FTIR spectra of Ca_2Al/X samples, X = Cl (a), VBS (b), and PSS (c). The spectra of VBS (d) and PSS (e) are displayed for comparison. The positions of the stretching S═O and of the vibration S−Φ are visualized by dashed lines (see text).

3.1.3. FTIR Study. To reinforce this idea of a strong interaction between VBS molecules and the inner surface of the sheets, FTIR analyses were performed. Such an interaction should induce a slight distortion of the SO_3 polyhedron, resulting in changes in frequency for the ν(S═O) symmetric and antisymmetric vibration bands. These bands appear at 1050 and 1190 cm^{-1} for VBS, respectively (Figure 4). For the polymer PSS, a slight change is observed for ν_{sym} (1038 cm^{-1}). Once VBS is intercalated, these vibration bands are shifted to lower frequency: $\Delta \approx 10$ cm^{-1} for $\nu_{antisym}$ and $\Delta \approx 15$ cm^{-1} for ν_{sym}. This downshift in frequency for the stretching corresponds to a weakening of the S═O bond strength, suggesting the presence of an electrostatic binding between hydrocalumite host and guest molecules, probably through a hydrogen bond via the path S═O···H−O−metal. Though of smaller amplitude, the effect of VBS interacting with the inorganic layers is also visible on the $S-\Phi_{cyc}$ vibration band for it is shifted from 1138 to 1126 cm^{-1}. Finally, a shift of the OH stretching indicates also that the hydroxyl groups in the octahedral layers are engaged with SO_3^- groups (left part of Figure 4).[22]

On the other hand, for PSS intercalate, the effect is only observed on the stretching $\nu_{antisym}$. The lattice vibrations of the inorganic framework appear in the 400−800 cm^{-1} wavenumber domain.

3.2. Reaction of Polymerization. *3.2.1. Thermal Contraction of the Lamellar Structure.* XRD pattern of Ca_2Al/VBS after thermal treatment at 200 °C displays broader diffraction lines (00*l*) than that observed for the chlorine phase calcined at the same temperature, whereas the width of the peak (110) does not change significantly (Figure 5). This indicates for the hybrid phase a slight disorder in the stacking sequence induced by the thermal treatment without affecting the intralamellar organization.

The lamellar structure is contracted down to 1.54 nm (Δd of 0.23 nm). In comparison, the basal spacing of the pristine material is decreased down to 0.095 nm after similar thermal treatment.

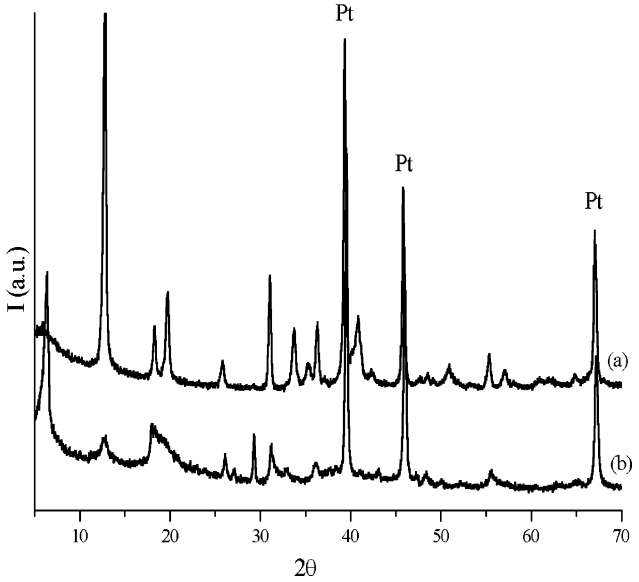

Figure 5. XRD patterns after thermal treatment at 200 °C of the samples Ca_2Al/X: (a) X = Cl; (b) X = VBS. The asterisk corresponds to the PSD response.

Such a strong contraction was already reported for in situ polymerization, as in the case of α,*β*-aspartate (from 1.10 to 0.90 nm)[17] and acrylate (from 1.36 to 1.26 nm)[23] into hydrotalcite-type compounds and ϵ-aminocaproic acid to nylon into a α-ZrP matrix (from 1.63 to 1.22 nm),[24] although in our case it suggests a highly constrained environment for the organic moiety.

3.2.2. VBS Polymerization. The in situ polymerization process is clearly evidenced by the ^{13}C CP-MAS spectrum of Ca_2Al/VBS after thermal treatment (Figure 6).

(22) Nakamoto, K. In *Infrared and Raman spectra of inorganic and coordination compound*, 4th ed.; Wiley: New York, 1986.

(23) Tanaka, M.; Park, I. Y.; Kuroda, K.; Kato, C. *Bull. Chem. Soc. Jpn.* **1989**, *62*, 3442. Rey, S.; Mérida-Robles, J.; Han, K.-S.; Guerlou-Demourgues, L.; Delmas, C.; Duguet, E. *Polym. Int.* **1999**, *48*, 277.

(24) Ding, Y.; Jones, D. J.; Maireless-Torres, P.; Rozière, J. *Chem. Mater.* **1995**, *7*, 562.

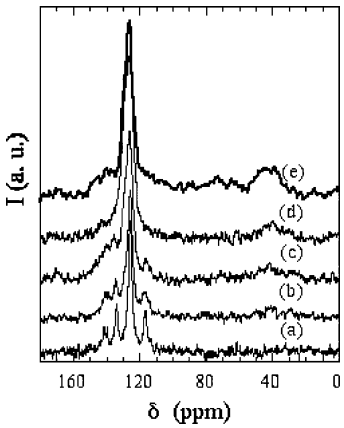

Figure 6. ^{13}C CP-MAS spectra of the sample Ca_2Al/VBS after thermal treatment at (a) 25, (b) 150, (c) 180, (d) 220, and (e) 250 °C.

The resonance peaks of the material resemble that of PSS (Figure 3a). In detail, the contribution associated with the vinyl bond (C^1) disappears and the formation of large humps located at ≈40−50 ppm is observed. It is characteristic of the resonance peaks of CH and CH_2, thus indicating that the molecules are polymerized. ^{13}C CP-MAS spectra recorded for lower temperatures display similar features with the progressive disappearance of the vinylic carbon atom until 220 °C (Figure 6).

FTIR analysis should also give evidence for the polymerization since this reaction is accompanied by the formation of CH, CH_2 bonds.

For the polymer PSS alone (Figure 4e), the vibration bands localized at 2926 and 2844 cm^{-1} correspond to the stretching of CH, antisymmetric and symmetric, respectively. They are slightly shifted when the polymer is incorporated between the layers of Ca_2Al (2921 and 2851 cm^{-1}) (Figure 4d). Even of small amplitude, these contributions are still present in the sample Ca_2Al/VBS after thermal treatment at 280 °C (2926 and 2856 cm^{-1}) (Figure 7). This result shows unambiguously that the polymerization has started.

3.3. Stability in Temperature. In situ high-temperature XRD measurements were carried out on Ca_2-Al/VBS. The diagrams at selected temperatures are presented in *static* (recorded after cooling at room temperature) or *dynamic* conditions (recorded at the applied temperature) (Figure 8). A reversible contraction of the lamellar structure is observed from room temperature to 150 °C. The same behavior was observed for Ca_2Al/Cl, but on a larger range of temperature (up to 250 °C), and was attributed to a reversible dehydration process.[7] The moisture present in air is enough to induce such a reversibility, while under an anhydrous atmosphere, the process is not reversible (Figure 9b); the values in both conditions are overlapping. Above 150 °C, the reversibility is lost, and the initial basal spacing is not recovered.

This deviation coincides with the ignition of the reaction of polymerization, as shown by the ^{13}C CP-MAS experiment (Figure 6). For temperature above 230 °C, the lamellar structure is irreversibly contracted. Surprisingly, the basal spacing increases then slightly, while the line (110) has disappeared completely. This may originate from the migration of some Al^{3+} cations from O_h to T_d coordination, as observed during the thermal treatment of Al-based LDH materials.[25,26] Consequently, we surmise that the loss of the intralayer order is mainly due to changes in the cation distribution accompanied by a migration of Al^{3+} cations toward the interlayer gap, thus enlarging the basal spacing. This effect is even more pronounced under N_2 treatment (Figure 9b). A conversion of Al coordination from O_h to T_d is observed in ^{27}Al NMR spectra for the sample Ca_2-Al/VBS during thermal treatment (Figure 10). After treatment at 300 °C, two lines are observed, one at ca. 13 ppm and the other at 75 ppm (chemical shift not corrected). The former is assigned to Al atoms in an octahedral environment (Al^{VI}) and the latter attributed

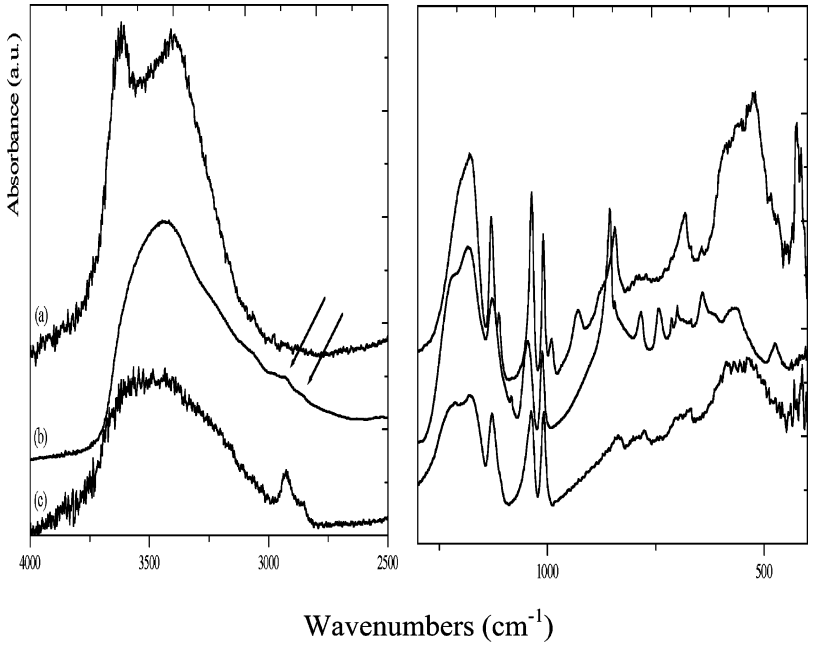

Figure 7. Selected regions of the FTIR spectrum for Ca_2Al/VBS at (a) 25 °C and (b) after treatment at 200 °C and (c) for Ca_2-Al/PSS.

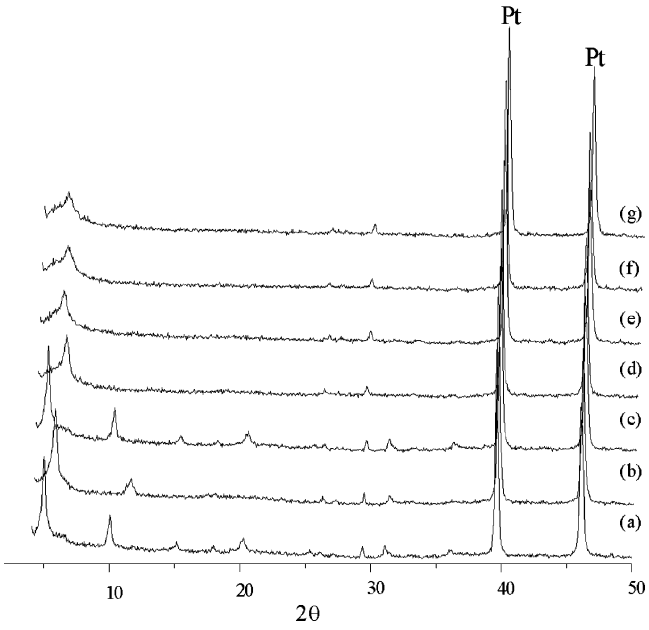

Figure 8. XRD patterns recorded at selected temperature (*dynamic* condition) and after cooling at room temperature (*static* condition) for the sample Ca_2Al/VBS: (a) 25 °C, (b) 80 °C dynamic, (c) 80 °C static, (d) 260 °C dynamic, (e) 260 °C static, (f) 280 °C dynamic, and (g) 280 °C static. The asterisk corresponds to the PSD response. The angular domain is enlarged for clarity.

to Al tetrahedral sites (Al^{IV}). At intermediate temperatures, an additional contribution is observed at ≈45 ppm, which may be ascribed to the presence of 5-fold coordinated Al atoms. To the best of our knowledge, such a coordination has never been reported in the LDH family, nor in calcined derivatives.

In comparison, the Ca_2Al/Cl sample presents more collective behavior with a rapid Al coordination change, whereas the process is spread in temperature for the Zn_2Al LDH sample.[19]

The nanocomposite Ca_2Al/PSS displays a quasi-constant basal spacing.[27] It can be pictured by a polymer holding together the lamellar structure, thus impeding any "breathing" behavior. The lamellar structure is maintained until a temperature of 450 °C, whereas the intralayer order is lost above 180 °C, lower than that for other parent organoceramics.[28]

3.4. Degradation in Temperature. Both organoceramics Ca_2Al/VBS and Ca_2Al/PSS start decomposing under air at 450 and 200 °C, respectively. $CaCO_3$ and $CaSO_4$ are observed at 550 °C in each case (Figure 11). At higher temperature, $CaCO_3$ transforms into CaO and the yeelimite $Ca_3Al_6O_{12}SO_4$ is also identified. The mayenite $Ca_{12}Al_{14}O_{33}$, which is formed during the thermal decomposition of the pristine material, is barely observed here after degradation of the sample Ca_2Al/PSS. The presence of sulfonate dictates the nature of the byproducts. This is even more evident when thermal treatments are carried out under a nitrogen atmosphere. Unlike in air, $CaSO_4$ is not observed. At higher temperature (T = 950 °C), calcium sulfide, CaS, is formed in the presence of CaO and either the mayenite for Ca_2Al/PSS or the yeelimite phase for Ca_2Al/VBS. An EDX analysis corroborates the presence of CaS.[27] The phases are less crystallized than those after treatment in air. To our knowledge, it is the first time that the formation of CaS from the hydrocalumite structure is reported.

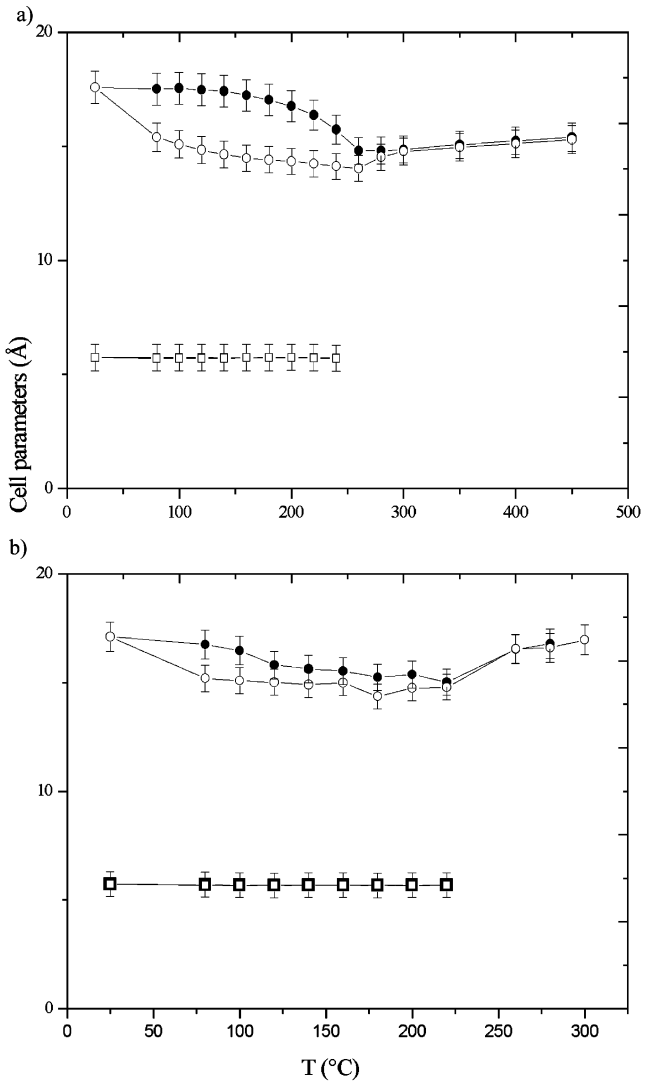

Figure 9. Variation of the cell parameters *a* (square) and of the basal spacing ($d = c/3$) (circle) for the sample Ca_2Al/VBS under (a) an air and (b) a nitrogen atmosphere. Open and black dots represent the data recorded under *dynamic* and *static* conditions, respectively. The points are linked as guide for the eyes.

3.5. Model for the in Situ Polymerization. A high charge density, that is, a small surface available per charge, corresponds to a large number of anions between the sheets. The hydrocalumite presents a charge density of 0.286 nm^2/e^-, and in the case of the chlorine form, the anionic exchange capacity is equal to 356 mequiv/100 g. All this gives a picture of anions literally packed between the sheets. Such high layer charge is considered as a drawback for an exfoliation reaction to proceed.[29]

(25) Belloto, M.; Rebours, B.; Clause, O.; Lynch, J.; Bazin, D.; Elkaim, E. *J. Phys. Chem.* **1996**, *100*, 8535.
(26) Rocha, J.; del Arco, M.; Rives, V.; Ulibarri, M. A. *J. Mater. Chem.* **1999**, *9*, 2499. Rey, F.; Fornes, V.; Rojo, J. M. *J. Chem. Soc., Faraday Trans.* **1992**, *88*, 2233.
(27) Supplementary electronic information.
(28) Moujahid, El M.; Besse, J.-P.; Leroux, F. *J. Mater. Chem.* **2003**, *13*, 258.
(29) Jacobson, J. *Comprehensive Supramolecular Chemistry: Colloidal dispersion of compounds with layer and chain structures*; Alberti, G., Bein, T., Eds.; Elsevier: Oxford, 1996; Vol. 7, p 315.

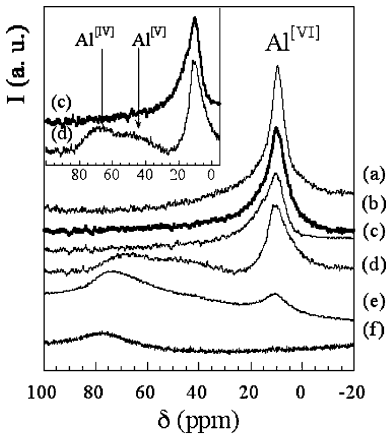

Figure 10. ^{27}Al MAS spectra of the sample Ca_2Al/VBS after thermal treatment at (a) 25, (b) 150, (c) 200, (d) 250, (e) 300, and (f) 350 °C. In the inset, the spectra of (c) and (d) are enlarged for clarity. The chemical shifts are not corrected from the second effect of the quadrupolar interaction.

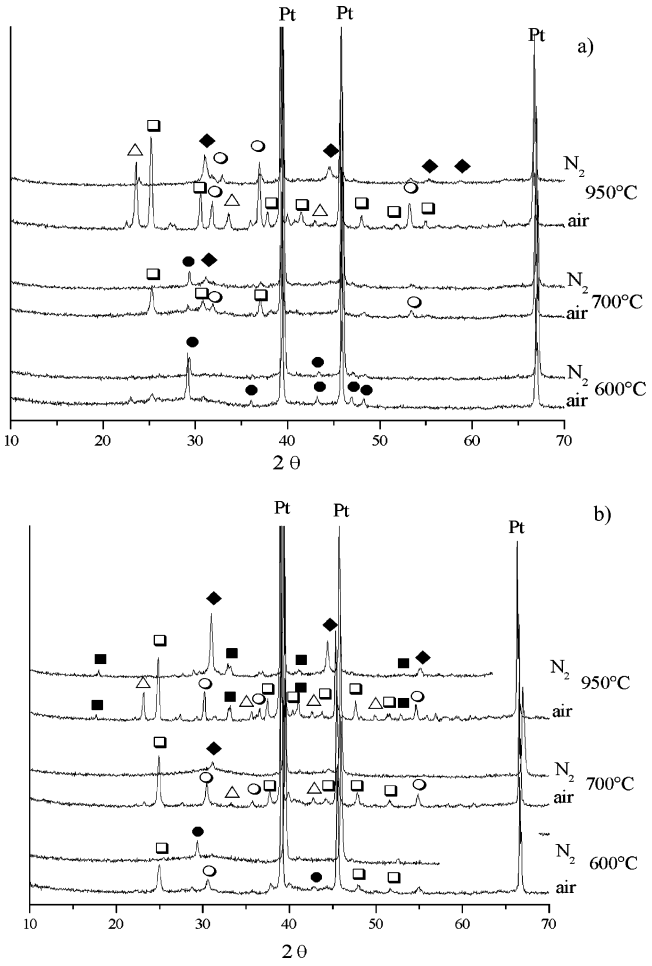

Figure 11. In situ XRD patterns recorded at selected temperatures for (a) Ca_2Al/VBS and (b) Ca_2Al/PSS samples under air or nitrogen atmospheres. Symbols: ○ CaO (PDF/48-1467), ● $CaCO_3$ (PDF/88-1809), □ $CaSO_4$ (PDF/80-0787), ■ $Ca_{12}Al_{14}O_{33}$, mayenite (PDF/48-1882), △ $Ca_3Al_6O_{12}SO_4$, yeelimite (PDF/16-0440), and ◆ CaS (PDF/77-2011).

In comparison, the charge density for smectites is ranging from 0.50 to 1.20 nm^2/e^-.

The change of the space group from $R\bar{3}$ for chloride intercalate to $C2/c$ for VBS intercalate is in total agreement with a bilayer arrangement of VBS anions in the interlamellar space, related by a 2-fold axis. The

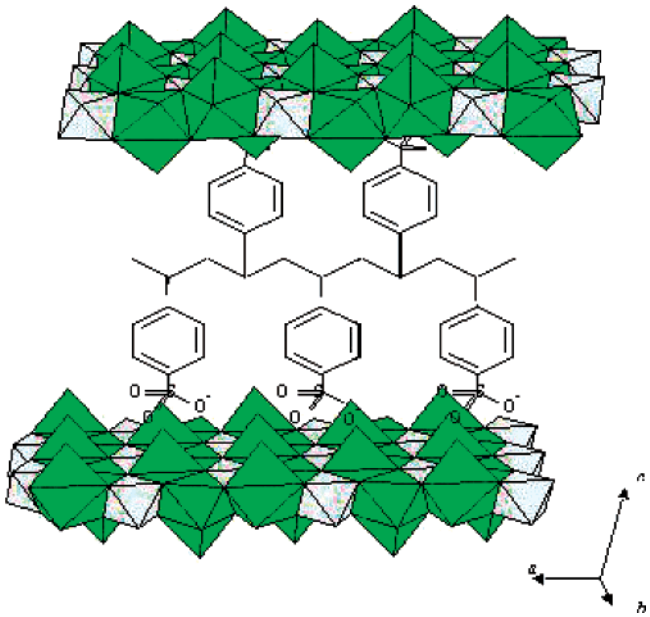

Figure 12. Schematic representation of the in situ polymerization process between hydrocalumite layers.

observed basal spacing d_{003} of 1.77 nm matches the value well considering the vertical size of VBS anions and the layer thickness of hydrocalumite host. This concordance may indicate that VBS anions are vertically oriented with respect to the hydroxide layers. The contraction in temperature induces a slight interdigitation or a tilted position.

Structural refinements reported elsewhere[7] in the $C2/c$ space group (a = 9.959 Å, b = 5.748 Å, c = 36.09 Å, γ = 104.61°) allow us to surmise that anions sites are distanced 9.96 Å along the a axis and 5.75 Å along the b axis. These distances are suitable for an in situ polymerization of syndiotactic type[30] running along the a axis as depicted in Figure 12.

4. Conclusion

Styrene-4-sulfonate and PSS molecules are found to be readily incorporated between the sheets of hydrocalumite via the coprecipitation method. The results gathered by FTIR and ^{13}C CPMAS techniques provide sheer evidence of a strong interaction of the guest molecule with the layers and of its subsequent polymerization after thermal treatment.

The strong structural cohesion arising from the charge density often considered as the limiting factor for polymer penetration is an advantage here to obtain a well-defined nanocomposite. Hydrocalumite host supplies a suitable arrangement for the polymerization. Indeed, the in situ polymerization of 4-styrene sulfonate in hydrocalumite gap may be viewed as a thermally activated endotactic process, reminiscent of the air-assisted reaction between poly(aniline) and FeOCl matrix.[31]

(30) Ayyagari, C.; Bedrov, D.; Smith, G. D. *Macromolecules* **2000**, *33*, 6194.
(31) Wu, C.-G.; DeGroot, D. C.; Marcy, H. O.; Schindler, J. L.; Kannewurf, C. R.; Bakas, T.; Papaefthymiou, V.; Hirpo, W.; Yesinowski, Y. P.; Liu, Y.-J.; Kanatzidis, M. G. *J. Am. Chem. Soc.* **1995**, *117*, 9229.

Hydrocalumite host structure forces the monomers to accommodate the anion site, and alternatively, PSS polymer forces the former to growth, explaining the difference in crystallinity between the two nanocomposites.

Acknowledgment. The authors would like to thank Joël Cellier for his help in acquiring the in situ XRD data.

CM031070I